

Exergoeconomic analysis of a conditioning system for captured CO₂: Costs of physical and chemical exergy

Rikke C. Pedersen ^{a,*}, Ebbe H. Jensen ^{b,c}, Brian Elmegaard ^a, and Jonas K. Jensen ^a

^a Technical University of Denmark, Dept. of Civil & Mechanical Eng., Kgs. Lyngby, DK

^b Technical University of Denmark, Dept. of Chemical Eng., Kgs. Lyngby, DK

^c Rambøll Danmark, København S, DK

*Corresponding Author: rikpe@dtu.dk

ABSTRACT

To keep the rise in global temperature below 1.5 °C, global greenhouse gas emissions should be reduced to net zero in 2050. Carbon Capture, Utilisation, and Storage (CCUS) is expected to play an important role in reducing emissions from the energy and industrial sectors. One important step of the CCUS value chain is the conditioning process, where the captured CO₂ is liquefied and purified before transportation. The conditioning process can be divided into several subprocesses, most of which contribute to both liquefaction and purification. Therefore, it is not straightforward to determine the costs associated with removing different types of impurities. In this study, the costs of achieving changes in the physical and chemical exergy are analysed through an exergoeconomic analysis. A detailed thermodynamic model and an economic analysis considering both capital investment and operational expenses were made. The overall costs of the system were found to be 25 €(t CO₂)⁻¹, of which 20 % were associated with reaching the correct quality of CO₂. The majority of these costs were related to the removal of water (16 % of total costs) while the direct costs of imposing constraints to incondensable gases for the given inlet composition were of minor significance (4 % of total costs). The results expand the knowledge of the economic effects from requirements downstream of the CCUS value chain.

1 INTRODUCTION

To keep the rise in global temperature below 1.5 °C, global greenhouse gas emissions should be reduced to net zero in 2050 (IPCC, 2022b). Energy and industrial processes accounted for a total of 78 % of global greenhouse gas emissions in 2016 (Ritchie & Roser, 2020), making these sectors of great importance in the green transition. Carbon Capture, Utilisation, and Storage (CCUS) is expected to play an important role in reducing emissions from the energy and industrial sectors and can even help achieve negative emissions through Direct Air Capture (DAC) and Bio-Energy Carbon Capture and Storage (BECCS) (IEA, 2021). However, to allow for large-scale deployment of CCUS, costs must be reduced in all parts of the value chain to make the technology economically feasible in the future (IPCC, 2022a).

It is expected that large infrastructures connecting several types of CO₂ sources and off-takers will be a necessity to fully utilise the potential of the technology and to gain economic scaling effects (Roussanaly *et al.*, 2021). However, this opens the question of which CO₂ quality should be allowed in such infrastructures (Kolster *et al.*, 2017). Therefore, it is important to understand how quality requirements impose economic drawbacks and benefits throughout the whole value chain. One essential step is the conditioning process (Figure 1), which ensures that the captured CO₂ complies with requirements from the transport operators and off-takers. The purpose of the conditioning process is to reduce the volume



Figure 1: Position of the liquefaction and purification process in the carbon capture value chain.

of the captured CO₂ and to remove impurities.

Several studies (Gong *et al.*, 2022; Pedersen, Rothuizen, *et al.*, 2023; Seo *et al.*, 2015) have investigated how the costs of conditioning CO₂ to a liquid state are affected by different feed gas and product conditions. They all find that higher product pressure reduces costs. However, the removal of impurities in the CO₂ are not considered. Deng *et al.* (2019) and Jensen *et al.* (2024) find that the costs of the conditioning process increase when impurities are present in the feed stream. Similar conclusions are achieved by Aspelund *et al.* (2006) for a lower product pressure.

During conditioning, the CO₂ is initially compressed while up to 80 % of the present water content is removed during intercooling (Jensen *et al.*, 2024). The CO₂ is then further dehydrated. Finally, the CO₂ can be liquefied while incondensable gases with higher volatility than CO₂ are simultaneously removed. An external chiller can be used to provide cooling below ambient temperatures needed for the dehydration and liquefaction process. This shows that several of the individual subprocesses of the conditioning system provide more than one service. Therefore, it can be a challenge to evaluate the direct economic effect of imposing different CO₂ qualities. One way to evaluate these is through an exergoeconomic analysis. Exergy analyses on CO₂ liquefaction plants are made by Chen and Morosuk (2021) and Muhammad *et al.* (2020, 2021) considering pure CO₂ as the feed. Pedersen, Ommen, *et al.* (2023) include water in the CO₂ while Aliyon *et al.* (2020) also include incondensable gases. Both studies perform an exergoeconomic analysis, but with the goal of identifying improvement potential for the overall system. Therefore, costs are not assigned to the different exergy elements, i.e. physical and chemical exergy.

In the present study, an exergoeconomic analysis was used to evaluate the costs associated with achieving each of the two services provided by the conditioning system, i.e. an increase of pressure and reduction of temperature to reach a liquid state, and to concentrate CO₂. This can aid the evaluation of how large a share of the conditioning costs are associated directly with purification and dehydration and how expensive it is to reach each of the two products. It can be useful for estimating the effects of imposing purity constraints on the CO₂ product.

2 METHODS

2.1 System description

The CO₂ entered the conditioning system in a gaseous state (1.5 bar, 30 °C) and was delivered in a liquid state (16 bar, -30°C). The CO₂ was assumed to be captured through post-combustion chemical absorption and should be purified from the inlet composition (Kemper *et al.*, 2014) to commercial specifications set out by Northern Lights JV DA (2024) for storage in a saline aquifer as given in Table 1.

The CO₂ conditioning system (see Figure 2) was of a typical type used for post-combustion chemical

Table 1: Molar concentrations of chemical components in the captured CO₂ feed gas (Kemper *et al.*, 2014) and requirement to the liquid product (Northern Lights JV DA, 2024).

	CO ₂ %	H ₂ O ppm	N ₂ ppm	O ₂ ppm	CO ppm	H ₂ S ppm	NH ₃ ppm
Feed gas	97.1	28700	486	29.1	9.71	0.971	4.86
Liquid product	≥ 99.81	≤ 30	≤ 50	≤ 10	≤ 100	≤ 9	≤ 10

capture plants at energy and chemical industrial sites and consisted of several distinct processes. The CO₂ feed gas was initially compressed through two-stage compression with intercooling while water was simultaneously condensed and removed in gas-liquid separators. The CO₂ was then dehydrated in a direct contact cooler (DCC), followed by further dehydration using an adsorption system with two columns. One column was used for drying while the second column was simultaneously regenerated using a fraction of the CO₂ stream. The dehydrated CO₂ stream entered the reboiler of a distillation column. The column was used to ensure that the final product stream complied with specifications for the incondensable gases. The CO₂ stream was condensed and the incondensable gases were separated in a gas-liquid separator and vented to the ambient. Finally, the CO₂ was subcooled and pumped to the product specifications. The overall process was divided into nine different control volumes, at which level the exergoeconomic analysis could be performed in a meaningful way without increasing the complexity of the calculations. These are indicated with coloured boxes in Figure 2.

A two-stage external chiller using R-744 as the working media (see Figure 3) was used to provide cooling at temperatures below ambient. The cooling for condensation and subcooling of the CO₂ stream was performed at the low-stage evaporator of the chiller. An evaporator at the intermediate pressure level was used to provide cooling for the DCC. Cooling water (CW) was used for process cooling above ambient temperatures namely during intercooling, aftercooling and adsorption dehydration.

2.2 Energy analysis

The CO₂ conditioning system was modelled in the chemical process modelling tool ProMax[®] 6.0.23032 using the Peng-Robinson equation of state (Peng & Robinson, 1976). The analysis was performed in steady-state applying energy balances to all components. Compressors were modelled using a polytropic

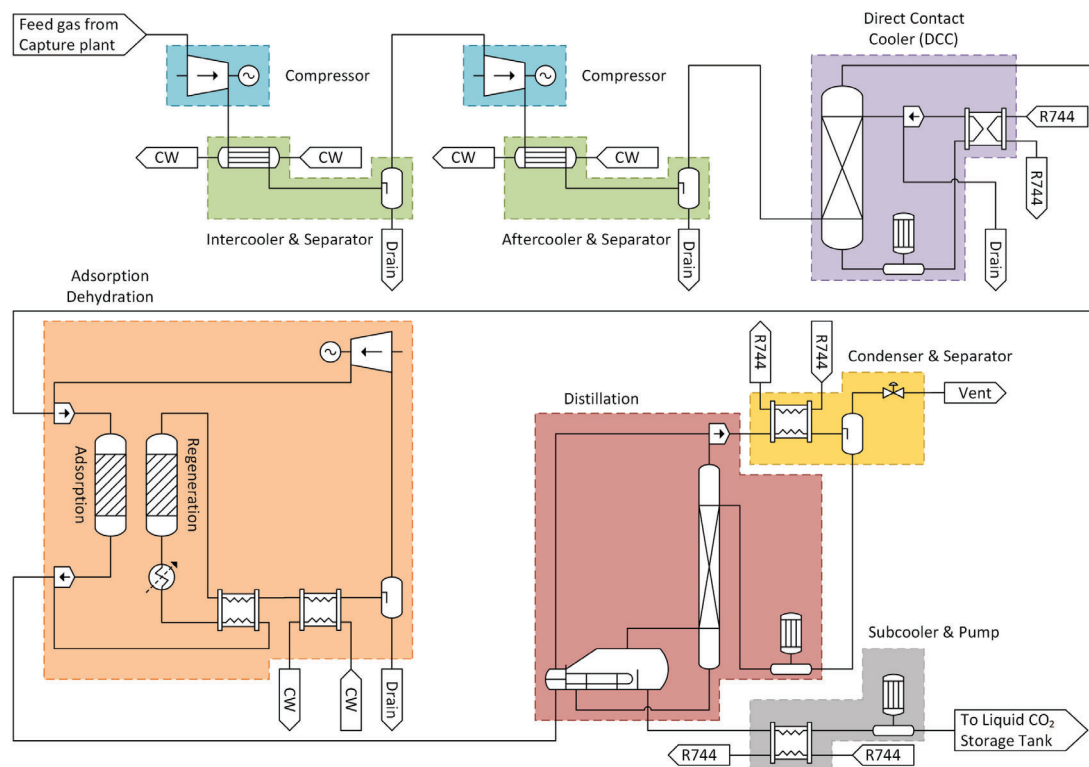


Figure 2: Process flow diagram of the conditioning system. The coloured boxes indicate the division of the nine control volumes considered in the exergoeconomic analysis. Arrows indicate entering and leaving material streams.

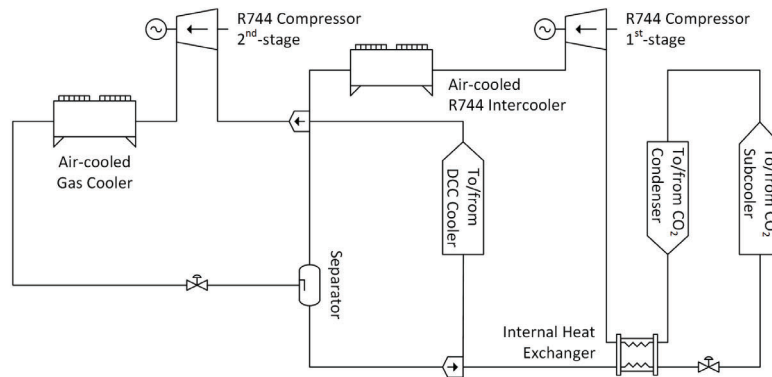


Figure 3: Process flow diagram of the two-stage R-744 chiller that provides cooling for the direct contact cooling, condensation, and subcooling processes.

efficiency, heat exchangers were modelled with an approach temperature, and pumps were modelled with an isentropic efficiency (see Table 2). Heat losses were neglected for all components (except the regeneration column) and pressure losses of 0.5 bar were included for heat exchangers. The DCC was modelled with an ideal column model with two stages, while the distillation column model was rate-based with ten stages. The adsorption drying column used zeolite 13X as the adsorbant. Further information about the modelling methodology can be found in Jensen *et al.* (2024).

2.3 Economic analysis

The size of each component was determined based on the size relations given in Table 3 and used as a basis for the economic analysis made by Jensen *et al.* (2024). Capital expenses were estimated for each component using the Enhanced Detailed Factor Method described by Aromada *et al.* (2021) and costs of reference components given by Woods (2007). The capital investment was annualised and discounted. Operational expenses were assumed to be constant on a yearly basis and included fixed operation and maintenance, salary to personnel, and consumption of adsorbant to the adsorption dehydration. The resulting capital investment and operational costs of each control volume and the external chiller are given in Table 4 for reference. For further information on the economic analysis see Jensen *et al.* (2024).

2.4 Exergy and exergoeconomic analysis

Exergy is a measure to gauge the potential for useful work that a system can deliver through a process where the system is brought to equilibrium with the surroundings, while heat transfer occurs only with the surroundings (Bejan *et al.*, 1996). In this study, the specific exergy (e) was divided into physical (PH) and chemical (CH) parts, respectively, as given in Equation (1). In this way, the exergy analysis can be used as a tool to compare the service of liquefying CO₂ to that of purifying CO₂ through the conditioning

Table 2: Parameters used in the model. For further information see Jensen *et al.* (2024).

Components	Parameter	Value	Source
CO ₂ 1 st and 2 nd Compressor		78 %	(Woods, 2007)
Ads. Dry. Compressor	Polytropic efficiency	65 %	(Woods, 2007)
R-744 1 st and 2 nd Compressor		70 %	NDA
Intercooler, Aftercooler, Ads. Dry. Condenser,		10 K	(Woods, 2007)
DCC Cooler, CO ₂ condenser, R-744 Internal HEX	Minimum temperature difference	5 K	NDA
R-744 Gas Cooler, R-744 Intercooler		15 K	(Woods, 2007)
Ads. Dry. Recuperator*		30 K	NDA
DCC pump, Distil. pump, Liquid CO ₂ Pump	Isentropic efficiency	60 %	(Woods, 2007)

*For remaining heat exchangers, the minimum temperature difference was given from the stream temperatures.

Table 3: Size factors and relations for each component type.

Component Type	Sizing Factor	Sizing Relation
Compressors	Power (\dot{W})	$\dot{W} = \dot{m}\Delta h$
Pumps	Volume flow rate (\dot{V}_{in})	$\dot{V}_{in} = \dot{m}/\rho_{in}$
Heat exchangers	Heat transfer area (A_{heat})	$A_{heat} = \dot{Q}/(U\Delta T_{lm})$
Gas-liquid separators	Product of height and diameter ($HD^{3/2}$)	$A_{cross} = \dot{V}_{gas}/u$, $D = \sqrt{4A_{cross}/\pi}$, Souders-Brown equation, $H/D = 3$
Columns	Product of height and diameter ($HD^{3/2}$)	Fair's correlation, $H = H_{packing} + H_{internals}$
Support tray	Diameter of column (D)	Fair's correlation
Structured packing	Volume (V)	$V = H_{packing}D^2\pi/4$

system. The restricted reference state was set to the surroundings (denoted as state 0) and defined as 15 °C and 1 atm, respectively. The chemical reference state was based on the model by Szargut *et al.* (1988) and the standard chemical exergy (e_0^{CH}) of each chemical component (n) was chosen accordingly. The reversible work associated with mixing effects was modelled assuming ideal mixtures (Bejan *et al.*, 1996) using the molar fractions (x) in the specific state point. The standard chemical exergy of the given mixture was weighted using the mass fractions (y) and the reversible work was converted to a mass basis using the molar weight of the mixture (M). By multiplying the specific exergy by the mass flow rate (\dot{m}), the exergy flow rates through the system are $\dot{E} = e \cdot \dot{m}$ for both physical and chemical parts.

$$e = \underbrace{(h - h_0) - T_0(s - s_0)}_{e^{PH}} + \underbrace{\sum_n (y_n e_{0,n}^{CH}) + \frac{RT_0 \sum_n (x_n \ln x_n)}{M}}_{e^{CH}} \quad (1)$$

The exergy destruction (D) rate occurring within the system was determined by applying exergy balances for each control volume as given in Equation (2) (Bejan *et al.*, 1996). Material streams exiting the control volumes without being further utilised within the system were considered as losses (i.e. cooling water, drainage and vent).

$$\sum \dot{E}_{in} = \sum \dot{E}_{out} + \dot{E}_D \quad (2)$$

On a system level, a physical and chemical product was defined. As the CO₂ was purified in the system, mass was lost through drainage and vented gas. Therefore, the products only concerned the change in specific exergy of the substream corresponding to the delivered mass flow rate of liquid CO₂. The definitions of products (P) and fuel (F) are given in Table 5.

The exergy was used as a basis for assigning costs to the liquefaction and purification parts of the process. The cost flow rates are given as the product of the specific cost of exergy (c) and the exergy flow rate:

Table 4: Cost elements of the system processes. From Jensen *et al.* (2024).

	Capital Investment [k€]	Operation & Maintenance [k€ y ⁻¹]
1 st CO ₂ Compressor	6214	381
Intercooler & Separator	775.7	32.1
2 nd CO ₂ Compressor	6223	382
Aftercooler & Separator	684.7	28.3
DCC	977.6	44.1
Ads. Dry.	1489	76.9
Distil.	2052	88.3
CO ₂ Condenser & Separator	163.5	6.76
Subcooler & Liquid CO ₂ Pump	100.9	5.82
External Chiller	12 920	764

Table 5: Flow rates of exergy products and fuel for the overall system.

\dot{E}_F	\dot{E}_P^{PH}	\dot{E}_P^{CH}
$\sum \dot{W} + \sum \dot{E}_{CW,in}$	$\dot{m}_{CO_2,liq}(e_{out}^{PH} - e_{in}^{PH})$	$\dot{m}_{CO_2,liq}(e_{out}^{CH} - e_{in}^{CH})$

$\dot{C} = c \cdot \dot{E}$ (Bejan *et al.*, 1996). Cost balances were applied to each control volume (see Table 6). For control volumes where the number of exiting exergy streams exceeds one, auxiliary cost equations were defined according to the approach by Lazzaretto and Tsatsaronis (2006) (see Table 6). The components in the external chiller were of more standard types, and the cost balances were made with the definitions detailed by Bejan *et al.* (1996), see also Pedersen, Ommen, *et al.* (2023).

In the intercooling and separation process (see Figure 2) the costs were allocated to the increase of chemical exergy within the control volume (CV) and the increase in physical exergy during the second compressor stage. This was done since the process assisted in the removal of water and reduction of irreversibilities within the second compressor. The costs were allocated according to the ratio between the two exergy products, as given in Equation (3).

$$\dot{C}_{aux,comp} = \frac{\dot{E}_{P,CV3}^{PH}}{\dot{E}_{P,CV2}^{CH} + \dot{E}_{P,CV3}^{PH}} (\Delta\dot{C}^{PH} + \dot{C}_{CW,in} + \dot{Z} - \dot{C}_{drain}) \quad (3)$$

The costs of loss streams of cooling water and air were defined as 0 €kJ⁻¹ in the analysis, and thus exergy costs were assigned directly to the product of the subprocesses involving these material streams. Costs were assigned to the losses of drainage and the vented gas, and these were assigned directly to the chemical exergy product on a system level. The definitions of cost rates of fuel and products for the overall system are given in Table 7.

To evaluate the economic value of the exergy destruction on the system level, it was assumed that the product rate is constant: $\dot{C}_D = c_F \cdot \dot{E}_D$ (Bejan *et al.*, 1996). Here, c_F is the average cost per unit of exergy

Table 6: Cost balances and auxiliary equations for each control volume.

Control volume	Cost balance	Auxiliary equation (F/P principle)
1 st Compressor	$c_{el}\dot{W} + \dot{Z} = \Delta\dot{C}^{PH}$	F: $c_{in}^{CH} = c_{out}^{CH}$
Intercooler & Separator	$\Delta\dot{C}^{PH} + \dot{C}_{CW,in} + \dot{Z} = \Delta\dot{C}^{CH} + \dot{C}_{drain} + \dot{C}_{aux,comp}$	F: $c_{drain} = c_{in}$, $c_{in}^{PH} = c_{out}^{PH}$
2 nd Compressor	$c_{el}\dot{W} + \dot{Z} + \dot{C}_{aux,comp} = \Delta\dot{C}^{PH}$	F: $c_{in}^{CH} = c_{out}^{CH}$
Aftercooler & Separator	$\Delta\dot{C}^{PH} + \dot{C}_{CW,in} + \dot{Z} = \Delta\dot{C}^{CH} + \dot{C}_{drain}$	F: $c_{drain} = c_{in}$, $c_{in}^{PH} = c_{out}^{PH}$
DCC	$\Delta\dot{C}^{PH} + \Delta\dot{C}_{ref} + c_{el}\dot{W} + \dot{Z} = \Delta\dot{C}^{CH} + \dot{C}_{drain}$	F: $c_{ref,in} = c_{ref,out}$, $c_{drain} = c_{in}$, $c_{in,PH} = c_{out,PH}$
Ads. Dry.	$\Delta\dot{C}^{PH} + \dot{C}_{CW,in} + c_{el}\dot{W} + \dot{Z} = \Delta\dot{C}^{CH} + \dot{C}_{drain}$	F: $c_{drain} = c_{in}$, $c_{in}^{PH} = c_{out}^{PH}$
Distil.	$\Delta\dot{C}_{gas}^{CH} + \Delta\dot{C}_{liq}^{PH} + c_{el}\dot{W} + \dot{Z} = \Delta\dot{C}_{gas}^{PH} + \Delta\dot{C}_{liq}^{CH}$	P: $\Delta\dot{C}_{gas}^{PH}/\Delta\dot{E}_{gas}^{PH} = \Delta\dot{C}_{liq}^{CH}/\Delta\dot{E}_{liq}^{CH}$, F: $c_{gas,out}^{CH} = c_{gas,in}^{CH}$, $c_{liq,out}^{PH} = c_{liq,in}^{PH}$
Condenser & Separator	$\Delta\dot{C}_{ref} + \dot{Z} = \Delta\dot{C}^{CH} + \Delta\dot{C}^{PH} + \dot{C}_{vent}$	P: $\Delta\dot{C}^{PH}/\Delta\dot{E}^{PH} = \Delta\dot{C}^{CH}/\Delta\dot{E}^{CH}$, F: $c_{ref,out} = c_{ref,in}$, $c_{vent} = c_{in}$
Subcooler & Liq. Pump	$\Delta\dot{C}_{ref} + c_{el}\dot{W} + \dot{Z} = \dot{C}^{PH}$	F: $c_{ref,out} = c_{ref,in}$, $c_{in}^{CH} = c_{out}^{CH}$

Table 7: Cost flow rates for the overall system.

\dot{C}_F	\dot{C}_P^{PH}	\dot{C}_P^{CH}
$\sum \dot{C}_{el} + \sum \dot{C}_{CW,in}$	$\dot{E}_{out}^{PH}(c_{out}^{PH} - c_{in}^{PH})$	$\dot{E}_{out}^{CH}(c_{out}^{CH} - c_{in}^{CH}) + \dot{C}_{L,vent} + \sum \dot{C}_{L,drain}$

fuel. It was assumed that the entering CO₂ feed gas was free of charge, hence $c_{in}^{CH} = c_{in}^{PH} = 0 \text{ €kJ}^{-1}$. The cost of the cooling water was set to be 1.86 €GJ^{-1} (determined from a cost balance of the auxiliary system), while the cost of electricity was 24 €GJ^{-1} or 87 €MWh^{-1} (Pedersen, Ommen, *et al.*, 2023).

A levelized cost (LC) per unit of liquefied and purified CO₂ was defined as given in Equation (4). It takes the overall system costs and divides it on a mass basis to the produced CO₂, i.e. the mass flow rate of liquid CO₂ leaving the system. Using the cost flow rates associated with the exergy product of liquefaction and purification, the levelized costs can be divided between the two services.

$$LC = \frac{\dot{Z} + \dot{C}_F}{\dot{m}_{CO_2,liq}} = \frac{\dot{C}_P}{\dot{m}_{CO_2,liq}} \quad (4)$$

3 RESULTS

3.1 Exergy

Only the state points of the CO₂ product stream entering and leaving the control volumes (see Figure 2) were considered in the analysis. The exergetic and exergoeconomic results for these state points are shown in Table 8 together with the mass flow rates, temperatures, and pressure levels. Reaching the required liquid state of the CO₂ product was associated with an increase in the specific physical exergy. The feed gas contained little physical exergy (22.79 kJ kg^{-1}) as it was close to the conditions of the ambient. It was significantly increased throughout the system to reach the liquid product (201.1 kJ kg^{-1}). As expected, the major increases occurred during the initial two-stage compression reaching a specific exergy of 150.2 kJ kg^{-1} and during condensation resulting in 203.6 kJ kg^{-1} . Due to the presence of impurities during condensation, the saturation temperature of the mixture was reduced. Therefore, the condensation temperature of CO₂ was -33.6 °C while the final product was delivered in a subcooled state at -30.8 °C (see Table 8).

Purification of the CO₂ product stream was associated with a change in chemical exergy. The compositions of each of the state points considered are given in Table 9 for reference. The increase in specific chemical exergy throughout the system only amounted to 6.5 kJ kg^{-1} , indicating that the minimum work needed to purify the CO₂ to the given specifications was significantly lower than the minimum work needed to reach the liquid state at the required pressure level. The majority of the increase in specific chemical exergy occurred during removal of water from 445.0 kJ kg^{-1} to 451.2 kJ kg^{-1} , while a very small increase to 451.5 kJ kg^{-1} was associated with the removal of incondensable gases.

Table 8: Results for the CO₂ streams entering and leaving control volumes.

	\dot{m} kg s ⁻¹	T °C	p bar	e^{PH} kJ kg ⁻¹	e^{CH} kJ kg ⁻¹	\dot{E}^{PH} kW	\dot{E}^{CH} kW	c^{PH} €GJ ⁻¹	c^{CH} €GJ ⁻¹	\dot{C}^{PH} €h ⁻¹	\dot{C}^{CH} €h ⁻¹
Feed Gas	14.06	30.0	1.5	22.79	445.0	320.3	6255	0	0	0	0
To Intercooler	14.06	154.6	5.4	116.3	445.0	1635	6255	44.0	0	259	0
To 2 nd Comp.	13.98	40.0	4.9	86.71	447.2	1212	6252	44.0	0.091	192	2.05
To Aftercooler	13.98	167.8	17.5	181.5	447.2	2537	6252	58.9	0.091	538	2.05
To DCC	13.92	40.0	17.0	150.2	449.6	2091	6257	58.9	5.25	443	118
To Ads. Dry.	13.89	5.1	17.0	149.1	450.9	2070	6263	58.9	6.95	439	157
To Reboiler	13.89	12.2	16.8	148.3	451.2	2059	6265	58.9	8.68	437	196
To Condenser	14.38	-15.6	16.3	148.8	448.0	2141	6444	64.0	8.68	493	201
To Distil.	14.35	-33.6	16.3	203.6	448.3	2921	6432	99.7	8.79	1050	204
To Subcooler	13.85	-25.9	16.4	199.2	451.5	2760	6255	99.7	10.4	991	234
Liq. Product	13.85	-30.8	16.0	201.1	451.5	2786	6255	101	10.4	1010	234

Table 9: Molar concentrations of chemical components in CO₂ streams entering and leaving control volumes.

	CO ₂ %	H ₂ O ppm	N ₂ ppm	O ₂ ppm	CO ppm	H ₂ S ppm	NH ₃ ppm
Feed Gas	97.08	28 700	486	29.1	9.7	0.971	4.86
To Intercooler	97.08	28 700	486	29.1	9.7	0.971	4.86
To 2nd Comp.	98.37	15 800	492	29.5	9.8	0.984	4.64
To Aftercooler	98.37	15 800	492	29.5	9.8	0.984	4.64
To DCC	99.44	5040	498	29.9	10.0	0.995	4.06
To Ads. Dry.	99.88	630	500	30.0	10.0	0.999	0.497
To Reboiler	99.94	29.0	500	30.0	10.0	1.00	0.494
To Condenser	99.31	28.0	6440	344	122	0.986	0.478
To Distil.	99.35	28.1	5990	326	115	0.987	0.479
To Subcooler	99.99	29.1	22.9	10.0	2.66	1.00	0.495
Liq. Product	99.99	29.1	22.9	10.0	2.66	1.00	0.495

Due to the significant increase in specific physical exergy, the flow of physical exergy of the CO₂ product stream also increased throughout the system, while the flow of chemical exergy did not change significantly. This was caused by losses of material streams associated with the removal of impurities. Therefore, the rate of exergy products on a system level only considered the change in exergy of the mass flow rate of produced CO₂ (13.85 kg s⁻¹) as specified in Table 5. The exergy product rates are given in Table 10. The total exergy product rate of the system amounted to 2560 kW with the physical exergy constituting the majority (96 %), resulting in an exergy efficiency of 24 % of the system. Approximately 40 % of the supplied exergy was destroyed in the system, while the remaining left the system through losses of which the majority was contained in the cooling water.

3.2 Economics

The specific cost of physical exergy was increased in the process steps associated with reaching higher pressure levels and temperatures below the reference state (see Table 8). The majority of the costs were added to the physical exergy during compression and intercooling reaching a specific cost of 58.9 €GJ⁻¹. Additional 5.1 €GJ⁻¹ were added during precooling in the reboiler, while a majority was again associated with the condensation reaching a cost of 99.7 €GJ⁻¹. Significantly lower costs were found for the chemical exergy for which the greatest cost increase was associated with the removal of water during aftercooling reaching 5.25 €GJ⁻¹. All costs of the direct contact cooler and adsorption dehydration process were assigned to the chemical exergy as these subprocesses were only present in the system to reach the required purity, resulting in an increased specific cost of chemical exergy to 8.68 €GJ⁻¹. The condensation process and release of the vented gas did not contribute significantly to the cost of chemical exergy, while the distillation process resulted in some cost increase to 10.4 €GJ⁻¹.

Both the flow and specific costs of the physical exergy were significantly greater than for the chemical exergy, resulting in a greater cost flow rate. Therefore, the largest share of costs within the system was associated with the increase in physical exergy. The cost flow rate of the chemical exergy product on a system level was corrected for the costs associated with losses through drainage and the vented gas. The costs of these material streams were added to the cost flow rate of the chemical exergy product amounting to 241 €h⁻¹ (see Table 10). Comparing the cost flow rates of these losses, the vented gas had a higher value. The gas contained more exergy and was released downstream in the system compared to the drainage, resulting in a greater cost accumulation. On a mass basis, the costs accumulated in the lost CO₂ throughout the conditioning system amounted to 0.045 €kg⁻¹. The cost flow rate of exergy destruction (270 €h⁻¹) was lower than the costs of owning the system ($\dot{Z} = 596$ €h⁻¹), meaning that the cost increase of the CO₂ product was primarily associated with non-exergy-related costs.

Table 10: Results of the exergoeconomic analysis for the overall system.

\dot{E}_P^{PH}	\dot{E}_P^{CH}	\dot{E}_F	$\dot{E}_{L,vent}$	$\dot{E}_{L,drain}$	$\dot{E}_{L,CW}$	$\dot{E}_{L,air}$	\dot{E}_D
kW	kW	kW	kW	kW	kW	kW	kW
2470	89.67	10450	18.35	10.22	3317	234	4308
\dot{C}_P^{PH}	\dot{C}_P^{CH}	\dot{C}_F	$\dot{C}_{L,vent}$	$\dot{C}_{L,drain}$	$\dot{C}_{L,CW}$	$\dot{C}_{L,air}$	\dot{C}_D
€ h ⁻¹	€ h ⁻¹	€ h ⁻¹	€ h ⁻¹	€ h ⁻¹	€ h ⁻¹	€ h ⁻¹	€ h ⁻¹
1010	241	655	4.80	1.97	0	0	270

The lifetime costs of the system were levelized and given per mass basis of the produced CO₂ in Table 11. When splitting the total costs of the system, it was found that approximately 80 % were associated with liquefaction while the remaining 20 % were assigned to purification. The results indicate, that up to 4.8 € (t CO₂)⁻¹ of the costs could be avoided if the CO₂ was not purified. In practice, this would likely not be achievable (see Section 4). The costs of purification could further be distributed to the removal of water (processes until the reboiler in Table 8) and removal of incondensable gases. Considering the development in chemical cost flows, the removal of water accounted for a total of 16 % of all costs in the system while the removal of incondensable gases only accounted for 4 %. This indicates, that the direct costs of imposing quality requirements on incondensable gases were insignificant to the overall system for the investigated inlet composition. Considering the dehydration processes, the direct contact cooling and adsorption drying were found to account for 3 % of the overall costs, respectively, while the costs of dehydration during the initial compression, intercooling, and aftercooling accounted for 10 %. Since the majority of the present water was removed during the initial compression, intercooling and aftercooling (see Table 9), it was relatively more expensive to make the deep gas dehydration with the DCC and the adsorption drying system.

4 DISCUSSION

The costs associated with dehydration and distillation were some of the lowest in the system, both in terms of irreversibilities and capital investment (see Table A1). If it was not required to purify the CO₂ product stream, these costs could be avoided. However, both the aftercooler and reboiler of the distillation column assisted in reducing the temperature of the CO₂ product stream. If these processes were removed, alternative processes would be needed or an increased load would be imposed on the external chiller. Similar conclusions could be made for the physical exergy. If there were no requirement on reaching a higher pressure and liquid state of CO₂, the compression processes and condensation would be redundant. However, it would require significantly more effort to remove the water at lower pressure levels and be more complicated to handle incondensable gases if they could not be removed through phase separation. Therefore, the results cannot be used to directly indicate the true costs of liquefaction and purification separately. However, they indicate the value of the two products achieved through the present system and the direct potential for cost reductions if the requirements to water and incondensable gases in the final product were relaxed.

The greatest cost contribution to the purification was associated with the aftercooler. In this process the CO₂ product stream was cooled at a temperature greater than ambient, making the component dissipative from a thermal exergy point of view. However, the process still aided in reaching a temperature level closer to the final value, compared to the exit temperature from the second compressor. An alternative

Table 11: Levelized costs of liquefaction and purification given in € per ton CO₂ produced.

LC _{total}	LC _{liquefaction}	LC _{purification}
25.1	20.3	4.8

approach could be to assign part of the costs associated with this process to the final physical product of the system, which would result in a larger cost share associated with reaching the liquid state. It can be difficult to determine how the costs should be weighted between the product of a subprocess (the small increase in chemical exergy) and the overall physical product. Therefore, this approach was not used.

The chiller supplied exergy in three of the subprocesses, namely to the direct contact cooler, the condenser, and the subcooler. The fuel supplied in the condenser was significantly higher (1089 kW, see Table A1) compared to that of the direct contact cooler (76 kW) and subcooler and pump (34 kW), for the latter two, electricity for the pump was also supplied as fuel. This indicates, that majority of the costs associated with the external chiller could be assigned to the product of condensation. As the exergy product associated with condensing the CO₂ was significantly greater than that associated with removal of incondensable gases, most of the chiller costs were assigned directly to the liquefaction.

5 CONCLUSION

An exergoeconomic analysis was made of a conditioning system to liquefy and purify a captured CO₂ stream from a state close to ambient with a molar fraction of 97.1 % CO₂ to a liquid of >99.8 % CO₂ at 16 bar and -30 °C. Investment and operational costs were throughout the system divided between liquefaction and purification i.e. physical and chemical exergy, respectively. The change in physical exergy of the product was significantly higher than that of the chemical exergy. Approximately 20 % of the system costs were associated with reaching the correct quality of CO₂ while the remaining 80 % were related to reaching the correct state. The purification costs could further be divided, indicating that approximately 4 % and 16 % of the total system costs were directly associated with the removal of the incondensable gases and water, respectively. The results show that liquefaction was responsible for the highest share of costs from a system perspective and that constraints on the incondensable gases did not contribute significantly to the overall costs for the given inlet composition. The study contributes to the knowledge of how quality requirements downstream of the CCUS value chain affect the costs of the conditioning process.

APPENDIX

Table A1: Results for the control volumes of subprocesses.

	\dot{E}_F kW	\dot{E}_P kW	\dot{E}_D kW	\dot{Z} € h ⁻¹	\dot{C}_F € h ⁻¹	\dot{C}_P € h ⁻¹	\dot{C}_D € h ⁻¹	$\dot{Z} + \dot{C}_D$ € h ⁻¹
1 st Compressor	1591	1314	276.5	120	138	259	24.1	144
Intercooler & Separator	331.5	31.23	300.3	13.1	75.8	2.05	68.7	81.8
2 nd Compressor	1594	1325	268.6	121	139	346	23.4	144
Aftercooler & Separator	335.1	33.15	302.0	11.6	105	116	94.2	106
DCC	76.13	17.76	58.37	17.0	21.8	38.8	16.7	33.7
Ads. Dry.	120.7	3.498	117.2	27.0	12.0	39.0	11.7	38.7
Distil.	208.4	126.2	82.16	35.1	59.5	94.5	23.5	58.5
Condenser & Separator	1089	783.0	305.5	2.76	555	558	156	159
Subcooler & Liq. Pump	34.29	25.67	8.620	1.91	17.4	19.3	4.38	6.29

NOMENCLATURE

Roman Letters

\dot{C}	Cost rate [€ s^{-1}]
\dot{E}	Exergy flow rate [kW]
\dot{m}	Mass flow rate [kg s^{-1}]
\dot{Q}	Heat transfer rate [kW]
\dot{V}	Volume flow rate [$\text{m}^3 \text{s}^{-1}$]
\dot{W}	Power [kW]
\dot{Z}	Cost flow rate of owning component [€ s^{-1}]
A	Area [m^2]
c	Average cost per exergy unit [€ kJ^{-1}]
D	Diameter [m]
e	Specific exergy [kJ kg^{-1}]
H	Height [m]
h	Specific enthalpy [kJ kg^{-1}]
M	Molar mass [kg kmol^{-1}]
s	Specific entropy [kJ (kg K)^{-1}]
T	Temperature [$^{\circ}\text{C}$]
U	Overall heat transfer coefficient [$\text{kW (m}^2\text{K)}^{-1}$]
u	Velocity [m s^{-1}]
V	Volume [m^3]

x Molar fraction [-]

y Mass fraction [-]

Greek Letters

ρ Density [kg m^{-3}]

ε Exergy efficiency [%]

Subscripts and Superscripts

n Chemical component

0 Reference state

CH Chemical

D Destruction

el Electricity

F Fuel

liq Liquid

lm Logarithmic mean

P Product

PH Physical

Abbreviations

CV Control volume

CW Cooling water

DCC Direct contact cooler

HEX Heat exchanger

LC Levelized costs [€ kg^{-1}]

REFERENCES

- Aliyon, K., Mehrpooya, M., & Hajinezhad, A. (2020). Comparison of different CO₂ liquefaction processes and exergoeconomic evaluation of integrated CO₂ liquefaction and absorption refrigeration system. *Energy Conversion and Management*, 211. <https://doi.org/10.1016/j.enconman.2020.112752>
- Aromada, S. A., Eldrup, N. H., & Øi, L. E. (2021). Capital cost estimation of CO₂ capture plant using enhanced detailed factor (EDF) method: Installation factors and plant construction characteristic factors. *International Journal of Greenhouse Gas Control*, 110. <https://doi.org/10.1016/j.ijggc.2021.103394>
- Aspelund, A., Mølnevik, M. J., & Koeijer, G. D. (2006). Ship transport of CO₂: Technical solutions and analysis of costs, energy utilization, exergy efficiency and CO₂ emissions. *Chemical Engineering Research and Design*, 84, 847–855. <https://doi.org/10.1205/cherd.5147>
- Bejan, A., Tsatsaronis, G., & Moran, M. (1996). *Thermal design & optimization*. John Wiley & Sons, Inc. [https://doi.org/10.1016/S0140-7007\(97\)87632-3](https://doi.org/10.1016/S0140-7007(97)87632-3)
- Chen, F., & Morosuk, T. (2021). Exergetic and economic evaluation of CO₂ liquefaction processes. *Energies*, 14. <https://doi.org/10.3390/en14217174>
- Deng, H., Roussanaly, S., & Skaugen, G. (2019). Techno-economic analyses of CO₂ liquefaction: Impact of product pressure and impurities. *International Journal of Refrigeration*, 103, 301–315. <https://doi.org/10.1016/j.ijrefrig.2019.04.011>

- Gong, W., Remiezowicz, E., Fosbøl, P. L., & von Solms, N. (2022). Design and analysis of novel CO₂ conditioning process in ship-based CCS. *Energies*, *15*. <https://doi.org/10.3390/en15165928>
- IEA. (2021). *Net zero by 2050* (4th revision). <https://www.iea.org/reports/net-zero-by-2050>
- IPCC. (2022a). Energy systems. *Climate Change 2022: Mitigation of Climate Change*.
- IPCC. (2022b). Mitigation pathways compatible with 1.5 °C in the context of sustainable development. *Global Warming of 1.5 °C: IPCC Special Report on Impacts of Global Warming*, 93–174. <https://doi.org/10.1017/9781009157940.004>
- Jensen, E. H., Pedersen, R. C., Løge, I. A., Dlamini, G. M., Neerup, R., Riber, C., Elmegaard, B., Jensen, J. K., & Fosbøl, P. L. (2024). The cost of impurities: A techno-economic assessment on conditioning of captured CO₂ to commercial specifications [Preprint]. *International Journal of Greenhouse Gas Control*. <https://doi.org/10.2139/ssrn.4774399>
- Kemper, J., Sutherland, L., Watt, J., & Santos, S. (2014). Evaluation and analysis of the performance of dehydration units for CO₂ capture. *Energy Procedia*, *63*, 7568–7584. <https://doi.org/10.1016/j.egypro.2014.11.792>
- Kolster, C., Mechleri, E., Krevor, S., & Dowell, N. M. (2017). The role of CO₂ purification and transport networks in carbon capture and storage cost reduction. *International Journal of Greenhouse Gas Control*, *58*, 127–141. <https://doi.org/10.1016/j.ijggc.2017.01.014>
- Lazzaretto, A., & Tsatsaronis, G. (2006). SPECO: A systematic and general methodology for calculating efficiencies and costs in thermal systems. *Energy*, *31*, 1257–1289. <https://doi.org/10.1016/j.energy.2005.03.011>
- Muhammad, H. A., Lee, B., Cho, J., Rehman, Z., Choi, B., Cho, J., Roh, C., Lee, G., Imran, M., & Baik, Y. J. (2021). Application of advanced exergy analysis for optimizing the design of carbon dioxide pressurization system. *Energy*, *228*. <https://doi.org/10.1016/j.energy.2021.120580>
- Muhammad, H. A., Roh, C., Cho, J., Rehman, Z., Sultan, H., Baik, Y. J., & Lee, B. (2020). A comprehensive thermodynamic performance assessment of CO₂ liquefaction and pressurization system using a heat pump for carbon capture and storage (CCS) process. *Energy Conversion and Management*, *206*. <https://doi.org/10.1016/j.enconman.2020.112489>
- Northern Lights JV DA. (2024). *Liquid CO₂ quality specifications*. chrome-extension://efaidnbmnmbicajpcgcglefndmkaj/<https://norlights.com/wp-content/uploads/2024/02/Northern-Lights-GS-co2-Spec2024.pdf>
- Pedersen, R. C., Ommen, T., Rothuizen, E., Elmegaard, B., & Jensen, J. K. (2023). Exergoeconomic analysis of a system for liquefaction and purification of captured CO₂. *36th International Conference on Efficiency, Cost, Optimization, Simulation and Environmental Impact of Energy Systems*, 148–159. <https://doi.org/10.52202/069564-0015>
- Pedersen, R. C., Rothuizen, E., Ommen, T., & Jensen, J. K. (2023). Technoeconomic optimisation of systems for liquefaction and purification of captured CO₂. *26th International Congress of Refrigeration*, 358–369. <https://doi.org/10.18462/iir.icr.2023.0707>
- Peng, D. Y., & Robinson, D. B. (1976). A new two-constant equation of state. *Industrial and Engineering Chemistry Fundamentals*, *15*, 59–64. <https://doi.org/10.1021/i160057a011>
- Ritchie, H., & Roser, M. (2020). *CO₂ and greenhouse gas emissions*. <https://ourworldindata.org/greenhouse-gas-emissions>
- Roussanaly, S., Berghout, N., Fout, T., Garcia, M., Gardarsdottir, S., Nazir, S. M., Ramirez, A., & Rubin, E. S. (2021). Towards improved cost evaluation of carbon capture and storage from industry. *International Journal of Greenhouse Gas Control*, *106*. <https://doi.org/10.1016/j.ijggc.2021.103263>
- Seo, Y., You, H., Lee, S., Huh, C., & Chang, D. (2015). Evaluation of CO₂ liquefaction processes for ship-based carbon capture and storage (CCS) in terms of life cycle cost (LCC) considering availability. *International Journal of Greenhouse Gas Control*, *35*, 1–12. <https://doi.org/10.1016/j.ijggc.2015.01.006>
- Szargut, J., Morris, D. R., & Steward, F. R. (1988). *Exergy analysis of thermal, chemical, and metallurgical processes*. New York: Hemisphere Publishing.
- Woods, D. R. (2007). *Rules of thumb in engineering practice*. Wiley-VCH Verlag GmbH & Co.